

# Large scale plane–mirroring in the cosmic microwave background WMAP5 maps

V.G.Gurzadyan<sup>1,2</sup>, A.A.Starobinsky<sup>3</sup>, T.Ghahramanyan<sup>1</sup>, A.L.Kashin<sup>1</sup>,  
H.G.Khachatryan<sup>1</sup>, H.Kuloghlian<sup>1</sup>, D.Vetruccio<sup>4</sup> and G.Yegorian<sup>1</sup>

<sup>1</sup> Yerevan Physics Institute and Yerevan State University, Yerevan, Armenia

<sup>2</sup> ICRA, ICRA, University “La Sapienza”, Rome, Italy

<sup>3</sup> Landau Institute for Theoretical Physics, Moscow, 119334, Russia

<sup>4</sup> University of Lecce, Lecce, Italy

Received (October 26, 2019)

## ABSTRACT

We continue investigation of the hidden plane-mirror symmetry in the distribution of excursion sets in cosmic microwave background (CMB) temperature anisotropy maps, previously noticed in the three-year data of the Wilkinson microwave anisotropy probe (WMAP), using the WMAP 5 years maps. The symmetry is shown to have higher significance,  $\chi^2 < 1.7$ , for low multipoles  $\ell < 5$ , while disappearing at larger multipoles,  $\chi^2 > 3.5$  for  $\ell > 10$ . The study of the sum and difference maps of temperature inhomogeneity regions, along with simulated maps, confirms its existence. The properties of these mirroring symmetries are compatible with those produced by the Sachs-Wolfe effect in the presence of an anomalously large component of horizon-size density perturbations, independent of one of the spatial coordinates, and/or a slab-like spatial topology of the Universe.

**Key words.** cosmology, cosmic background radiation, topology

## 1. Introduction

The properties of the CMB temperature anisotropy, as well as its polarization, are among the basic sources of information on cosmological parameters (de Bernardis et al. 2000; Spergel et al. 2007; Komatsu et al. 2008). Their tiny features, such as the local spikes in the multipoles power spectrum, deviation from the statistical isotropy, and non-Gaussianity signatures, may all be the result of various fundamental processes having occurred in the early Universe. Among the reported anomalies are the alignment of the principal (Maxwellian) vectors of low multipoles, the north-south power asymmetry, the southern anomalous cold spot, etc (see de Oliveira-Costa et al. 2004; Copi et al. 2004,2007; Schwarz et al. 2004; Eriksen et al. 2004,2007; Cruz et al. 2005; Morales & Saez 2008). In the present paper we continue the study of another deviation from statistical isotropy: the hidden partial plane-mirror symmetry in the distribution of CMB temperature fluctuations excursion sets, i.e. of one-connected pixel sets equal to and higher than the given temperature threshold (lower for negative thresholds) previously found in the WMAP 3-years temperature maps (Gurzadyan et al. 2007b). We use the WMAP 5-years data (Hinshaw et al. 2008), not only to confirm the mirroring effect found in WMAP3 maps while studying the inhomogeneities in the distribution of the excursion sets, but also to reveal its other properties. By inquiring into the dependence of the mirror symmetry on the angular scale, we show that the effect has the highest significance at low multipoles  $\ell < 5$  and that it quickly disappears at higher multipoles.

Similarly, the study of the sum and difference maps of temperature inhomogeneity regions provides additional

insight into the mirroring. Namely, when the sum and difference maps are created via reflection of one of the maps, as it should be for mirrored images, anisotropic properties of excursion sets do survive, while they disappear if the sum map is created without reflection. Difference maps from independent radiometers (A-B) have been used to test the role of scan inhomogeneities and noise (Gurzadyan et al. 2007b). The signal-to-noise ratio for the studied excursion sets is about 4:1 and the excursion sets in (A-B) map do not show any specific property observed in the sum (A+B) map. The negligible role of the noise was also checked using the foreground reduced maps available in <http://lambda.gsfc.nasa.gov/product/map/current/>. Although contamination of a Galactic or interplanetary origin at these multipoles certainly cannot be excluded, following Gurzadyan et al (2007b), in the last section we discuss which properties of the Universe might be responsible for this effect, if it had a cosmological origin.

## 2. Distribution of excursion sets

For this analysis we used the 94 GHz (3.2mm) W-band WMAP 5-year maps, due to their offering the highest angular resolution (beam width of FWHM=0°.21) and lowest contamination by synchrotron radiation of the Galaxy (Bennett et al. 2003). The role of the Galactic disk was minimized via exclusion of the equatorial belt  $|b| < 20^\circ$ .

Algorithms for studying the excursion sets have been described in (Gurzadyan et al. 2005; Gurzadyan et al. 2007a) in connection with the study of the ellipticity in excursion sets in the Boomerang and WMAP, and earlier for COBE maps (Gurzadyan & Torres 1997). The definition of

the centers and of the geometrical characteristics of the excursion sets are based on rigorous procedures, e.g. the Cartan theorem for the conjugation of the maximally compact subgroups of Lie groups. The distribution of the centers of the excursion sets obtained via those algorithms were obtained for various pixel count and temperature-threshold interval sets and the center of these  $N$  centers was obtained:  $x(\text{center}) = \sum x_i/N$ ,  $y(\text{center}) = \sum y_i/N$ .

Inhomogeneities in the distribution of the excursion sets at the temperature interval  $\Delta T = 90 \mu K$  within  $|T| = 45 \mu K$  are concentrated around almost antipodal points centered at

$$l = 94^\circ.7, \quad b = 34^\circ.4 \quad (CE_N);$$

$$l = 279^\circ.8, \quad b = -29^\circ.2 \quad (CE_S).$$

At higher temperature interval limits the excursion sets are merged and lose their identity. The methodical novelty here is that we consider the excursion sets within a temperature interval  $[-T, T]$  with respect to the mean CMB temperature, instead of excursion sets in the slice around a fixed  $T$ . Namely, *the symmetry appears at the sum of slices but not in each of them*. This is analogous to the appearance of the Great Wall as a result of the sum of slices of large scale galaxy surveys.

Comparing these positions to those of the Maxwellian vectors of the lowest multipoles of CMB, it was shown that  $CE_N$  and  $CE_S$  are located close to one of the vectors of multipole  $\ell = 3$ , shifting towards the equator when increasing the temperature interval. During this shift, the mirror symmetry is approximately maintained, while the patterns of the excursion sets around  $CE_N$  and  $CE_S$  mirror each other with  $\chi^2 = 0.7 - 1.5$ .

Neither  $CE_N$  and  $CE_S$  are close to the positions of the sum of the multipoles vectors with  $\ell = 2 - 8$ , the modulus of each vector weighted by  $1/(\ell+1)$ . The position of  $CE_S$  is not close to that of the cold spot (Cruz et al. 2005).

### 3. Mirroring versus multipoles

We now investigate the multipole dependence of the mirroring. We study it using the method of gradually removing multipoles, defined by the coefficients  $a_{\ell m}$  of the temperature fluctuations expansion into spherical harmonics:

$$\frac{\Delta T_\ell(\hat{n})}{T} = \sum_{m=-\ell}^{\ell} a_{\ell m} Y_{\ell m}(\hat{n}). \quad (1)$$

The functions ‘‘anafast’’ and ‘‘synfast’’ of Healpix (Gorski et al. 2005) were used, and the WMAP5 94 GHz (W channel) dataset was analyzed. We checked that the temperature anisotropy can be represented as

$$\frac{\Delta T(\theta, \phi)}{T} = \left( \frac{\Delta T}{T} \right)_{\text{mirr}} + \left( \frac{\Delta T}{T} \right)_{\text{non-mirr}} \quad (2)$$

where the first, mirrored term dominates at certain (low) multipoles, while the second, non-mirrored term becomes the main one at other (higher) multipoles. Such partial mirroring does not imply planarity, i.e. the dominance of multipoles with  $|m| = \ell$ . Instead, for the first term on the right hand side of Eq. (2), all  $a_{\ell m}$  with an even value of  $\ell - m$  may be non-zero.

To quantify the degree of mirroring in (Gurzadyan et al. 2007b), the drift of the centers of the symmetries with respect to the dipole apexes vs the temperatures for each hemisphere was studied. The confidence levels defined as  $\chi^2 = (\sum_i^N (Y_{1i} - Y_{2i})^2)/(N - \text{DOF})$  (where  $Y_{1i}, Y_{2i}$  are the distances to the northern and southern dipole apexes, respectively, and  $N \simeq 30$  is the number of steps,  $\text{DOF} = 2$ , for the compared curves) have been evaluated, i.e. the departure from being identical (see Fig. 4 in (Gurzadyan et al. 2007b), as well as Figs. 5 and 6 there for the distances to the multipole vectors). Here we evaluate the analogous confidence levels but for the maps split over multipoles. Figure 1 shows the plots for the excursion sets of more than 50 pixel counts vs the multipole numbers where the points of given  $\ell$  indicate that multipoles smaller than  $\ell$  are cancelled. The red line there represents the best polynomial fit, while the dashed lines correspond to smoothed error bars. The plot shows that the mirroring effect has its highest significance at low multipoles,  $\chi^2 < 1.7$  for  $\ell < 5$ , and it weakens monotonically for higher ones; i.e.  $\chi^2 > 3.5$  at  $\ell > 10$ . For comparison, we also show the same dependence obtained using the WMAP 3-year W-maps (Fig. 2). Similar dependence occurs for larger excursion sets (Fig. 3). Figure 4 shows confidence levels for the mirroring effect when one of the mirrored regions (the northern, see below) is replaced by a simulated, statistically isotropic Gaussian map. For the latter, first, the maps for the given multipoles were obtained from the real map, then, for the resulted multipole maps, isotropic Gaussian maps were generated using the mean and the  $\sigma$  of each map.

Then, to probe the mirroring further, we constructed and compared the sum and the difference maps of regions  $(l, b)$ :  $[10^\circ, 170^\circ]$ ,  $[20^\circ, 90^\circ]$ ;  $[190^\circ, 350^\circ]$ ,  $[-20^\circ, -90^\circ]$ , respectively centered on  $CE_N$  and  $CE_S$ , using two procedures: (a) with rotation on the angle  $\pi$ , i.e. keeping the mirror symmetry; (b) without this rotation. The number of the excursion sets surrounding  $CE_N$  and  $CE_S$  are given in Fig. 5. The angular distances of  $CE_N$  and  $CE_S$  from the CMB dipole direction vs the temperature threshold are shown in Figs. 6a and 5b for the mirrored (i.e. with rotation) and non-mirrored sums and difference maps, respectively; the continuous and dashed lines denote the sum and difference maps, respectively. In Fig. 6b, the same dependence is plotted for a simulated statistically isotropic map, too (the upper dot-bar curve). Note that, while a difference map (A-B) obtained using data from different radiometers but from the *same* region of the sky contains mainly noise and no signal, when we deal with *different* sky regions, the difference map should result in another map that is not very different from the sum map. Indeed, Figs. 6a and b clearly indicate that the similarity in the temperature independence of the distance from the dipole for the non-mirrored sum map and the simulated map is obvious – in both maps there is no breaking of statistical isotropy. This differs crucially from the temperature dependence of this distance in the case of the mirrored sum and difference maps (Fig. 6a), thus confirming the existence of a partial mirror symmetry of the regions of  $CE_N$  and  $CE_S$ .

### 4. Conclusions and discussion

We have analyzed the scale dependence of partial mirror symmetry in the distribution of excursion sets, as previ-

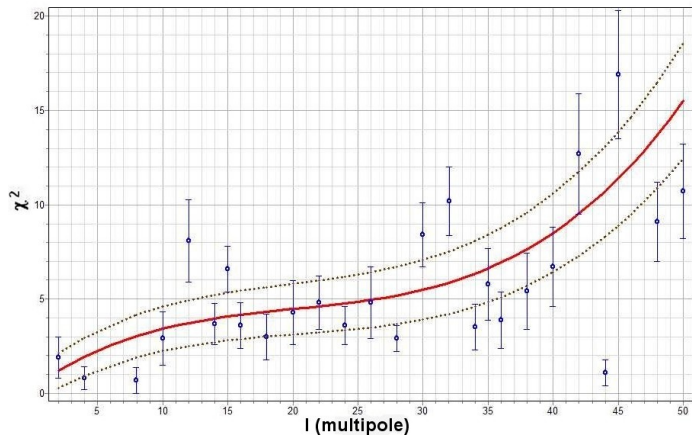


**Fig. 1.** Statistical significance of the mirroring of patterns of excursion sets with more than 50 pixel counts around the centers  $CE_N$  and  $CE_S$  vs the multipole number  $\ell$  for the WMAP 5-year 94 GHz temperature maps.

ously found in the WMAP3 maps, with a nearly antipodal location of symmetry centers. Studies used the WMAP5 W-band maps, and the results obtained using WMAP5 and WMAP3 data agree. The centers lie close to one of the  $\ell = 3$  multipole Maxwellian vectors, but not close to the sum of multipoles vectors up to  $\ell = 8$  (Gurzadyan et al. 2007b). Also they are close to the ecliptic pole and are nearly orthogonal to the CMB dipole apexes. They are moving towards the Galactic equator with the increase in the temperature threshold interval.

This symmetry appears to be a large-angle effect, i.e. it is stronger at low multipoles and it weakens rapidly for larger  $\ell$ : its statistical significance is quantified by  $\chi^2 < 1.7$  at  $\ell < 5$  and  $\chi^2 > 3.5$  at  $\ell > 10$ . The symmetry was also tested using the following procedure: the sum map of the symmetry regions was obtained first, via rotation over  $\pi$ , as is usually the case for mirrored images, and then without such a rotation. The clear mirroring in the first case and its complete absence in the second case make the case for a partial mirror symmetry stronger.

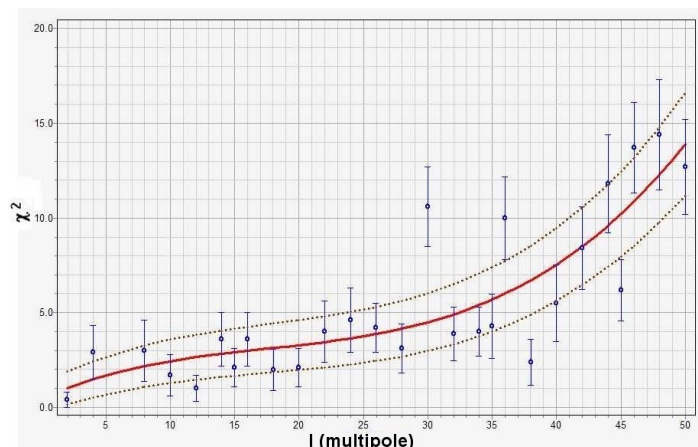


**Fig. 2.** The same as in Fig. 1, but for the WMAP 3-year maps.

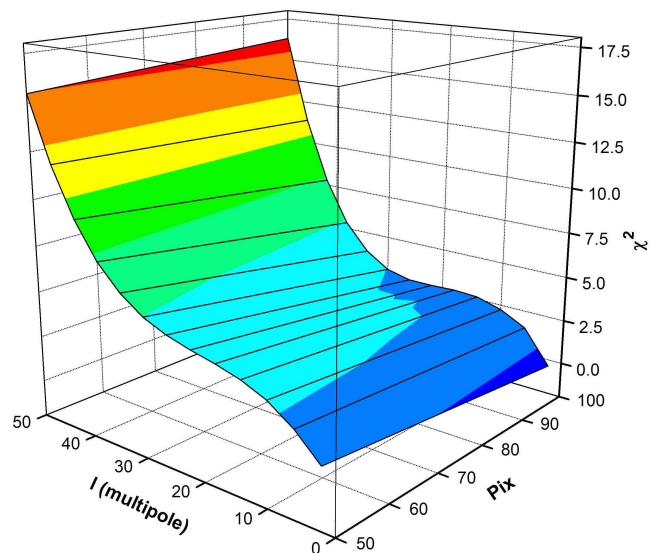


**Fig. 3.**  $\chi^2$  dependence as in Fig. 1, but now both vs the multipole number and the number of pixel counts of the excursion sets.

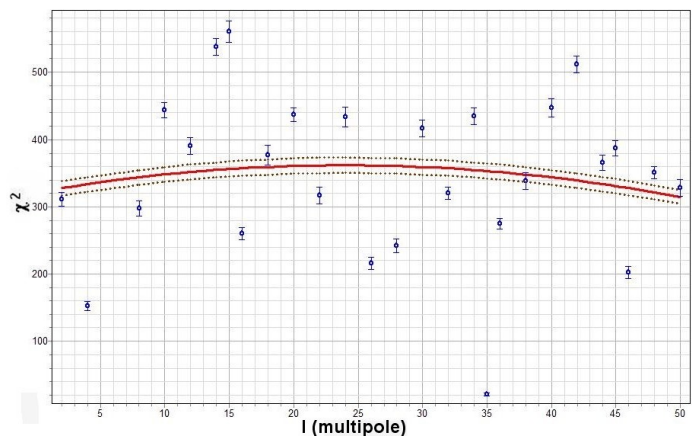


**Fig. 4.**  $\chi^2$  when one of the symmetry regions is replaced by a simulated statistically isotropic map.

Turning to the origin of this symmetry, an unknown interplay of interplanetary and Galactic foregrounds or another unspecified non-cosmological contribution to the low multipoles certainly remains a possibility. If, however, it has a cosmological origin, then a signature of the simplest non trivial,  $T^1$ , spatial topology of the Universe is among the options, as discussed in Gurzadyan et al (2007b). For this topology, the points with coordinates  $z$  and  $z+L$  are identified where  $z$  is one of the spatial coordinates. Such a model may be also considered as a limiting case of the Universe with compact flat spatial sections having the  $T^3$  topology if the identification scales  $L_1, L_2$  along two other spatial coordinates are much more than  $L$  – the slab topology (for early papers on a non trivial spatial topology of the Universe, see Zeldovich (1973), Sokolov & Schwartzman (1975), Sokolov & Starobinsky (1975), Fang & Sato (1983)). Note that, one should not expect any mirror symmetry, even a partial one, for comparable topological scales  $L \sim L_2, L_3$ .

As shown in Starobinsky (1993), for this  $T^1$  topology, a large-angle pattern of a CMB temperature anisotropy has just the form (2). The first term on its right hand side has the exact mirror symmetry with respect to the  $(x, y)$ -plane. It originates from the Sachs-Wolfe effect at the last scattering surface from density perturbations that do not depend on  $z$ . The second term represents a remaining part of anisotropy and does not have any symmetry at all. However, for  $a_0L$  on the order of  $R_{hor}$  or slightly more, where  $a_0 = a(t_0)$  is the present scale factor of a Friedmann-Robertson-Walker cosmological model, the latter term should somehow be suppressed since the Sachs-Wolfe contribution to it from the last scattering surface comes from perturbations having wave vectors with  $|\mathbf{k}| \geq 2\pi/L$ . That is why one expects the total large-angle pattern of  $\Delta T/T$  to have an *approximate* mirror symmetry in this case.<sup>1</sup>

More generically and not connected with a non trivial spatial topology of the Universe, such an approximate mirror symmetry at large angles arises when the large-scale  $z$ -independent part of density perturbations inside the last scattering surface is anomalously large. In all these cases, the rms amplitude of the first term on the right hand side of Eq. (2) quickly becomes negligible compared to the second one with the growth of  $\ell$ . Weakening of the mirroring symmetry for higher values of  $\ell$  found in Sect. 3 is in a good agreement with this theoretical prediction and may be considered as an additional argument for the reality of the mirroring effect.

Until now, searches for the mirroring effect of the form (2) or directly for the  $T^1$  topology gave negative results (see e.g. de Oliveira-Costa et al. 1996; de Oliveira-Costa et al. 2004; Cornish et al. 2004), raising the lower limit on the physical topological scale  $a_0L$  to  $\sim R_{hor} = 14$  Gpc. The numerical value is given for the standard  $\Lambda$ CDM cosmological model with  $\Omega_m = 0.3$ ,  $\Omega_\Lambda = 0.7$ . However, for higher values of  $a_0L$  this topology is not excluded. This

<sup>1</sup> Note the other effect worsening the symmetry at large angles (low multipoles): a contribution from the integrated Sachs-Wolfe effect at small redshifts due to a cosmological constant (first calculated in (Kofman & Starobinsky 1985)) or dynamical dark energy.

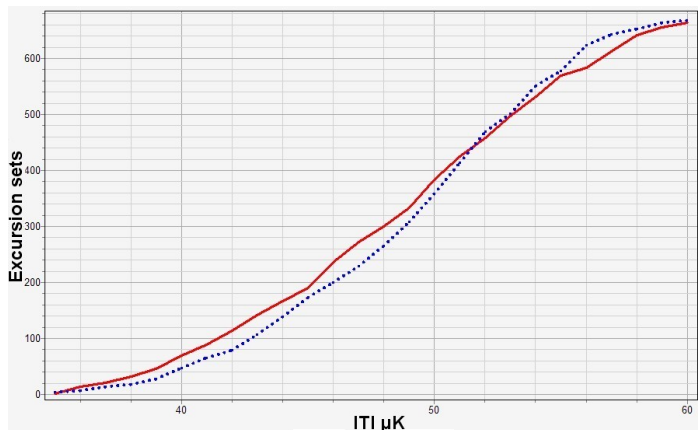


**Fig. 5.** The number of excursion sets with more than 100 pixels vs the temperature threshold within the regions centered on  $CE_N$  and  $CE_S$  (dashed line) for the WMAP 5-year 94 GHz temperature maps.

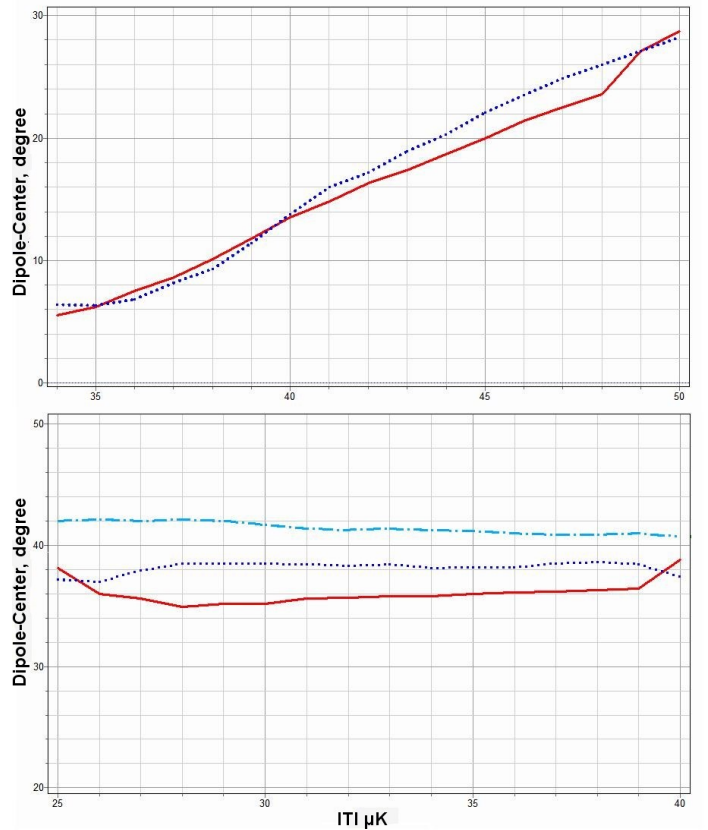


**Fig. 6.** Distances of  $CE_N$  and  $CE_S$  from the CMB dipole vs temperature for the sum and difference maps centered on  $CE_N$  and  $CE_S$ . (a) The sum and difference (dashed) maps obtained via rotation by the angle  $\pi$  in one of the maps (to keep the mirror symmetry); (b) no mirroring rotation performed for the sum and difference (dashed) maps; for comparison, the case of simulated isotropic maps is shown (dot-bar curve).

follows already from the fact that the much more restrictive cubic  $T^3$  topology ( $L = L_1 = L_2$ ) with  $a_0L > R_{hor}$  is still considered as a viable possibility; see the recent papers (Aurich et al. 2007; Aurich 2008), where an inconclusive evidence for the latter case with  $a_0L \approx 1.15R_{hor}$  is presented. This shows that topological explanation of the partial mirror symmetry investigated in this paper is possible. From our analysis, it is still too early to speak about the value of  $L$ , since the secure separation of CMB temperature fluctuations into a mirrored and non-mirrored parts needs higher resolution maps. Also, a non-topological (though still cosmological) explanation of such an effect is possible, as pointed out above. In this respect, see the recent papers (Gurzadyan & Kocharyan 2008) where it was shown that voids can act as hyperbolic lenses in a spatially flat Universe, producing specific signatures in CMB temperature fluctuations. Future observational data will help solve these problems.

Shortly before submission of this manuscript, a paper appeared (Groeneboom & Eriksen 2008) where CMB statistical anisotropy of an axial type was studied with the preferred axis very close to the one defined by our  $CE_N - CE_S$  direction.

## 5. Acknowledgments

We thank the referee for valuable comments. We are grateful to Paolo de Bernardis for continuous advice and help. AAS was partially supported by the Research Program “Astronomy” of the Russian Academy of Sciences and by grant LSS-4899.2008.2. YPI team was partially supported by INTAS. HKh was supported by the IRAP PhD program.

## References

- R. Aurich, arXiv:0803.2130 [astro-ph]  
 R. Aurich, H.S. Janzer, S. Lustig and F. Steiner, *Clas. Quant. Grav.* **25** (2008) 125  
 C.L. Bennett, R.S. Hill, G. Hinshaw *et al.*, *Astroph. J.Suppl.* **148** (2003) 97  
 P. de Bernardis, P.A.R. Ade, J.J. Bock *et al.*, *Nature* **404** (2000) 955  
 C.J. Copi, D. Huterer, D.J. Schwarz and G.D. Starkman, *Phys.Rev. D* **75** (2007) 023507  
 C.J. Copi, D. Huterer and G.D. Starkman, *Phys. Rev. D* **70**(2004) 043515  
 N.J. Cornish, D.N. Spergel, G.D. Starkman and E. Komatsu, *Phys. Rev. Lett.* **92** (2004) 201302  
 M. Cruz, E. Martinez-Gonzalez, P. Vielva and L. Cayon, *Mon. Not. Roy. Astron. Soc.* **356** (2005) 29  
 H. Eriksen, A.J. Banday, K.M. Gorski and P.B. Lilje, *Astroph. J.* **612** (2004) 633  
 H. Eriksen, A.J. Banday, K.M. Gorski *et al.*, *Astroph. J.* **660** (2007) L81  
 L.Z. Fang and H. Sato, *Comm. Theor.Phys.* **2** (1983) 1055  
 K.M. Gorski, E. Hivon, A.J. Banday, B.D. Wandelt, F.K. Hansen, M. Reinecke, M. Bartelmann, *Astroph. J.* **622**(2005) 759; <http://healpix.jpl.nasa.gov/>  
 N.E. Groeneboom and H.K. Eriksen, arXiv:0807.2242 [astro-ph]  
 V.G. Gurzadyan, P. de Bernardis, G. De Troia *et al.*, *Mod. Phys. Lett. A* **20** (2005) 813  
 V.G. Gurzadyan, C.L. Bianco, A.L. Kashin *et al.*, *Phys.Lett. A* **363** (2007a) 121  
 V.G. Gurzadyan and A.A. Kocharyan, arXiv:0805.4279 [astro-ph]; arXiv:0807.1239 [astro-ph]  
 V.G. Gurzadyan, A.A. Starobinsky, A.L. Kashin *et al.*, *Mod. Phys. Lett. A* **22** (2007b) 2955  
 V.G. Gurzadyan and S. Torres, *Astron. Astroph.* **321** (1997) 19  
 G. Hinshaw, J.L. Weiland, R.S. Hill *et al.*, arXiv:0803.0732[astro-ph]  
 L.A. Kofman and A.A. Starobinsky, *Sov. Astron. Lett.* **11** (1985) 271  
 E. Komatsu, J. Dunkley, M.R. Nolta *et al.*, arXiv:0803.0547 [astro-ph]  
 J.A. Morales and D. Saez, arXiv:0802.1042 [astro-ph]  
 A. de Oliveira-Costa, G.F. Smoot and A.A. Starobinsky, *Astroph. J.* **468** (1996) 457  
 A. de Oliveira-Costa, M. Tegmark, M. Zaldarriaga and A. Hamilton, *Phys. Rev. D* **69** (2004) 063516  
 D.J. Schwarz, G.D. Starkman, D. Huterer and C.J. Copi, *Phys. Rev. Lett.* **93** (2004) 221301  
 D.D. Sokolov and V.F. Schwartzman, *Sov. Phys. – JETP* **39** (1975) 196  
 D.D. Sokolov and A.A. Starobinsky, *Sov. Astron.* **19** (1975) 629  
 D. Spergel, R. Bean, O. Dore *et al.*, *Astroph. J. Suppl.* **170** (2007) 377  
 A.A. Starobinsky, *JETP Lett.* **57** (1993) 622  
 Ya.B. Zeldovich, *Comm. Astroph. Space Phys.* **5** (1973) 169